ACS APPLIED MATERIALS & INTERFACES

www.acsami.org

Research Article

Facile Mechanochemical Functionalization of Hydrophobic Substrates for Single-Walled Carbon Nanotube Based Optical Reporters of Hydrolase Activity

Abbas Elhambakhsh, Mohaddeseh Abbasi, Cole R. Dutter, Marshall D. McDaniel, Brett VanVeller, Andrew C. Hillier, and Nigel F. Reuel*

Cite This: *ACS Appl. Mater. Interfaces* 2024, 16, 62547−62556

Read Online

ACCESS | Metrics & More | Article Recommendations | Supporting Information

ABSTRACT: Single walled carbon nanotubes (SWCNT) have recently been demonstrated as modular, near-infrared (nIR) probes for reporting hydrolase activity; however, these have been limited to naturally amphipathic substrate targets used to noncovalently functionalize the hydrophobic nanoparticles. Many relevant substrate targets are hydrophobic (such as recalcitrant biomass) and pose a challenge for modular functionalization. In this work, a facile mechanochemistry approach was used to couple insoluble substrates, such as lignin, to SWCNT using L-lysine amino acid as a linker and tip sonication as the mechanochemical energy source. The proposed coupling mechanism is ion pairing between the lysine amines and lignin carboxylic acids, as evidenced by FTIR, NMR, SEM, and elemental analyses. The limits of detection for the lignin−lysine−SWCNT (LLS) probe were established using commercial enzymes and found to be 0.25 ppm (volume basis) of the formulated product. Real-world use of the LLS probes was shown by evaluating soil hydrolase activities of soil samples gathered from different corn root proximal locations and soil types. Additionally, the probes were used to determine the effect of storage temperature on the measured enzyme response. The modularity of this mechanochemical functionalization approach is demonstrated with other substrates such as zein and 9-anthracenecarboxylic acid, which further corroborate the mechanochemical mechanism.

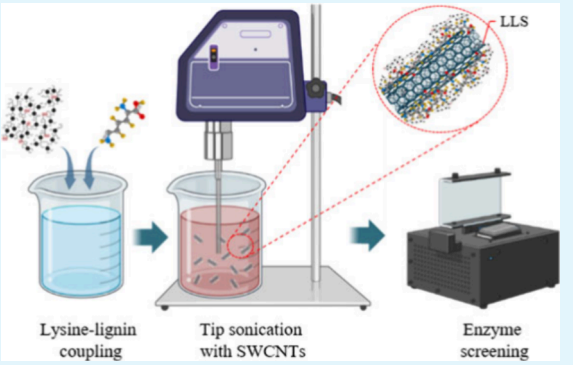

KEYWORDS: *hydrolase, soil enzymes, mechanochemistry, activity measurement, carbon nanotubes, lignin*

1. INTRODUCTION

Hydrolases are an important class of enzymes that catalyze the deconstruction of complex molecules such as carbohydrates and proteins.[1] They are central to metabolism in all organisms, recycling bulk materials to provide building blocks for new growth. Moreover, they have found many practical industrial applications as biocatalysts in detergents, foods, materials, and environmental management[2−4] with a global market valued greater than US$4 billion in 2020.[2,5] In soil, hydrolytic enzymes like ligninases, proteases, cellulases, etc., are responsible for converting organic compounds into crucial nutrients required for microbial and plant growth including phosphorus, sulfur, and nitrogen in mineralized states.[6,7] The detection of these enzymes is key to evaluating soil health[5−7] as well as a new technique to anticipate the available and required nutrients in farmland soils.[8−10]

There are various methods using carbon nanotubes and other nanoparticle-based technologies to detect enzyme activity, such as electrochemical sensors,[11] field-effect transistors (FETs),[12] and piezoelectric sensors.[13] While these approaches have demonstrated the strengths of dynamic monitoring, applicability for a wide range of targets, and flexibility for integration into portable devices, their fabrication and use can sometimes limit end use, especially when applying them to high throughput enzyme screening campaigns in standard micro well-plate formats or microdroplet assays. In contrast, solution-based optical probes (absorbance or fluorescence) can readily be manipulated by automated pipettors and integrated into large screening campaigns.

Fluorometric and colorimetric assays are powerful tools for measuring the activity of hydrolases due to their high sensitivity and specificity.[18] The most well-known fluorometric methods include fluorescent substrates,[19] coupled enzyme assays,[20] fluorescent probes,[21] fluorescent labeling,[22] and time-resolved fluorescence (TRF).[23] Most of these methods rely on

Received: August 15, 2024
Revised: October 22, 2024
Accepted: October 22, 2024
Published: October 30, 2024

https://doi.org/10.1021/acsami.4c13800
ACS Appl. Mater. Interfaces 2024, 16, 62547−62556

smaller proxies of the target substrates, which can lead to poor screening results when validated against actual substrates. Fluorescent single-walled carbon nanotube (SWCNT) based probes that are wrapped in actual enzyme substrates have been proposed to overcome this limitation.[24] The hydrolase attacks the wrapping, exposing the SWCNT to the solvent and thereby altering the fluorescence of the nanotube. Thus, when observing the nIR signal from the SWCNT probe, we measure the decrease in the signal as a measure of relative activity. For further description of the photophysical effects of molecular interactions with SWCNT, we suggest the following seminal reviews.[24,25] With many complex substrates, such as lignin, multiple enzymes are needed to degrade the material by using oxidative and hydrolytic mechanisms. For instance, lignin peroxidase cleaves the aromatic rings and C−C linkages in non-phenolic lignin units, breaking down the complex lignin structure. Manganese peroxidase, on the other hand, generates phenoxy radicals through Mn^{3+} ions, leading to lignin depolymerization. Laccase oxidizes phenolic hydroxyl groups, producing phenoxy radicals that destabilize lignin's structure, facilitating its degradation. As a result, all these enzymes function by degrading the lignin-wrapped groups on SWCNTs, ultimately exposing the surface of the SWCNTs to the solvent and self-aggregation, which reduce the number of exciton pathways and decrease the observed fluorescence.

Our group and others have shown the potential of this approach by screening activities of many different hydrolases.[16,26−31] One critical limitation to SWCNT based probes for hydrolase screening to date is the use of naturally occurring amphipathic substrates, such as soluble proteins such as bovine serum albumin (BSA) to screen protease activity. More hydrophobic substrates, like many relevant biomass substrates found in soil, are capable of associating with SWCNT but are unable to make a stable dispersion due to lack of polar side groups; this makes the probe incompatible with the aqueous buffer-based screening used in enzyme testing.

A few strategies can be employed to overcome the challenges of hydrophobic substrates. In some cases, chemical modifications to the substrate can be found commercially, such as carboxymethyl cellulose, as a suitable substrate for cellulase screening. However, this is not a viable option for custom probes developed on specific field-derived substrates. Chemical functionalization of insoluble substrates relies on organic, solvent-based procedures, which require skill and safe handling and often result in low yields that are difficult to purify. For instance, although much effort has been made, the extremely cross-linked and chemically heterogeneous structure of lignin has remained a significant challenge for its functionalization and solubilization.[32] Furthermore, current lignin functionalization techniques require high operating temperatures (about 160 °C)[33] and can also be highly affected by various parameters such as the source and pretreatment of lignin, pH, lignin concentration, and the type of solvent used.[34] An alternative approach to solvent-based chemistry is the use of mechanochemistry to associate the target hydrophobic substrates with an appropriate hydrophilic side group. These techniques mainly use vibration (e.g., bead mills) as the source of energy and depend on overcoming significant lattice energies, ensuring particle mixing, and activating the surface.[35,36] Mechanochemical techniques[37,38] have been used in material synthesis[36,39,40] and organic chemistry[41,42] creating metal−organic frameworks (MOFs),[43−45] coordination polymers,[46,47] and distinctive pharmaceutical cocrystals.[48−50] They have also been employed in the covalent oxygen functionalization of SWCNTs[51] and as a grafting strategy to produce organo-soluble SWCNTs to prepare flexible conductors.[52] In addition to their facile nature, mechanochemical methods have the benefit of an improved environmental footprint due to elimination of organic solvent use and minimal waste generation.[53,54]

Herein we evaluate the use of sonication-based mechanochemistry to functionalize target hydrophobic substrates to use in suspending SWCNT as optical probes for screening hydrolytic enzymes. Lignin, zein, and anthracene compounds are used as test substrates, and a mechanochemical mechanism is proposed based on metrology and observations. The mechanochemically modified lignin is then used to suspend SWCNT and make probes that are applied to assessment of lignin degrading activity of commercial and soil enzymes.

2. METHODS AND MATERIALS

2.1. Sensor Synthesis. The LLS sensor was synthesized in two steps. As the first step, 20 mg of L-lysine (MW 164.21, Thermo Fisher Scientific Chemicals, 39665-12-8) was added to 2 mL of water and homogenized by applying intensive ultrasonic irradiation (2 W with Qsonica Q125, 1/8 in. probe) for 90 min while the solution was cooled by a cooling system. Subsequently, 20 mg of lignin (Sigma, 370959) was added to the solution, and the sonication was continued for 90 min. Following this, the solution was centrifuged for 15 min (11180*g*) to separate the unreacted substances. It is worth mentioning that there was no observed sedimentation, showing a significant change in the hydrophilic properties of lignin.

LLS solution was prepared by sonicating (2 W, in an 5 mL centrifuge tube) the mixture of 1 mg of SWCNT (Sigma (6,5) chirality, ≥95% carbon basis (≥95% as carbon nanotubes), 0.78 nm average diameter, Product #773735), 2 mL of lignin−lysine, and 2 mL of water for 90 min to achieve a black solution. The solution was then centrifuged for another 15 min to ensure that the LLS solution was stable, and there was no sedimentation. Finally, the LLS probe was diluted five times to obtain a final concentration of 0.02 wt % SWCNT solution for enzyme activity screening experiments.

2.2. NIR Experiment. As stated, the LLS solution was initially diluted five times and then dispensed into a 96-well black-walled plate with a volume of 80 μL. The well plate was immediately placed on an nIR well-plate scanner (custom build, described in REF[16,26]) to conduct the enzyme activity screening. Scanning began and continued until a relatively constant signal was observed for the LLS solution. Next, a volume of 20 μL of water containing enzyme and/or deactivated enzyme and/or pure water was added to the sensors, and screening continued until a discernible difference in the trend of the line graphs was detected. Details about the scanning procedure, which was carried out using Python scripts, and the subsequent data analysis in MATLAB can be found in our previous work.[16]

2.3. Enzyme Extraction from Soil Samples. After the soil samples were collected, they were individually mixed with deionized (DI) water in a mass ratio of 1:2 and stirred for 30 min. Subsequently, a specific amount of liquid was separated and centrifuged (11180*g*) for 10 min, and the water containing the enzymes was collected from the clear supernatant at the upper part of the liquid phase. Controls were also prepared by heating the water−enzyme solution to 90 °C for 45 min.

3. RESULTS AND DISCUSSION

3.1. Chemistry and Material Preparation. Sonication of the SWCNT with either lysine or lignin alone led to unstable dispersions with pronounced sedimentation, as the lignin is too hydrophobic alone to stay in suspension and the lysine is not hydrophobic enough to electrostatically associate with the SWCNT. Sonication of lignin and lysine together prior to

https://doi.org/10.1021/acsami.4c13800
ACS Appl. Mater. Interfaces 2024, 16, 62547−62556

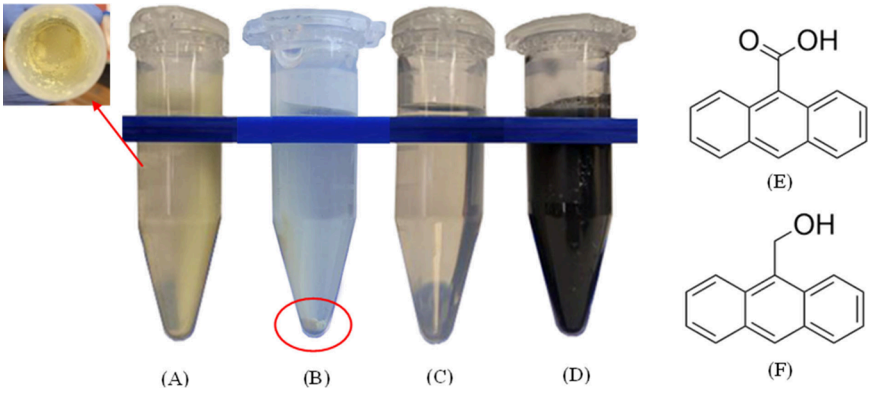

Figure 1. Images of (A) 9A-COOH, (B) 9A-OH-lysine, (C) 9A-COOH-lysine, (D) 9A-COOH-lysine-SWCNT, (E) 9A-COOH chemical structure, and (F) 9A-OH chemical structure.

Scheme 1. Proposed Mechanism of Mechanochemical Functionalization of Lignin with Lysine to Create an Amphipathic Substrate Capable of Dispersing SWCNT in Water[a]

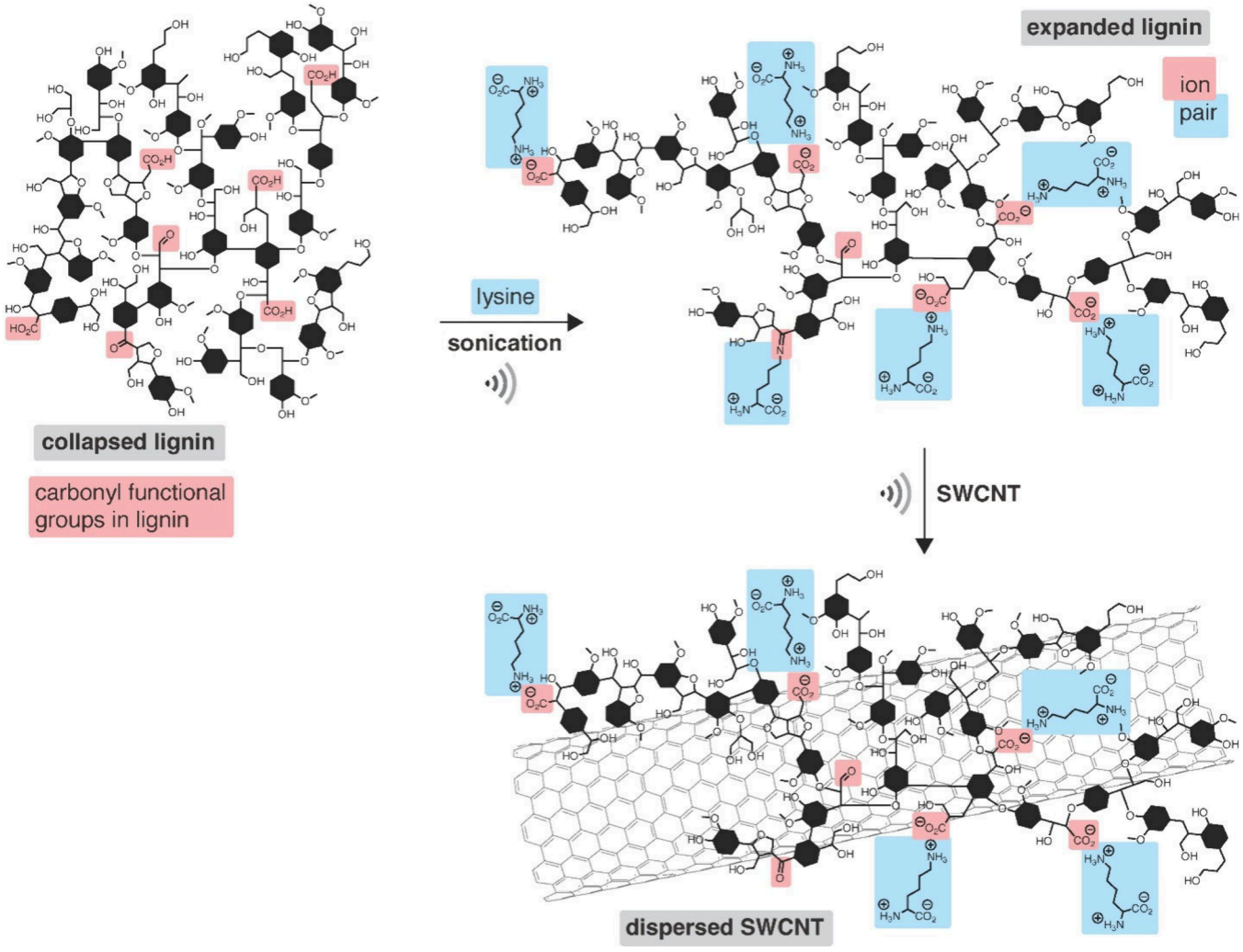

[a]The mechanical energy exfoliates the lignin and largely induces ion pairing as well as some transient imine formation between lysine and the carbonyl functional groups in lignin. More information about the elemental analysis and FT-IR spectra of lignin−lysine and SEM images is available in the Supporting Information, Sections S3, S4, and S5, respectively.

sonication with the SWCNT, however, led to a stable solution even after prolonged centrifugation. This result indicated mechanochemical conjugation between the lignin and lysine in the first sonication step, creating a wrapping capable of dispersing the SWCNT surface but remaining charged enough to stay in suspension. Indeed, after extensive dialysis of the lignin−lysine material to remove free lysine, elemental analysis revealed a 10-fold increase in the weight percentage of nitrogen

https://doi.org/10.1021/acsami.4c13800
ACS Appl. Mater. Interfaces 2024, 16, 62547−62556

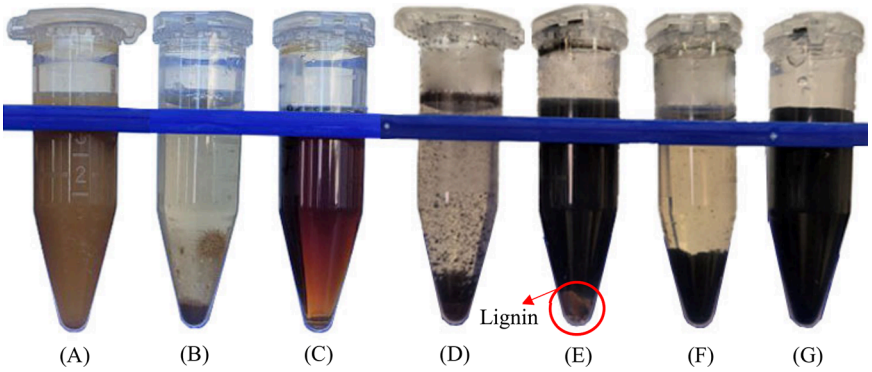

Figure 2. Images of (A) bare lignin after sonication and before centrifugation, (B) lignin after sonication and centrifugation, (C) lignin−lysine after sonication and centrifugation, (D) LLS before sonication, (E) lignin−SWCNT after sonication and centrifugation, (F) lysine−SWCNT after sonication and centrifugation, and (G) LLS after sonication and centrifugation.

in the material (Table S3). We hypothesized that some kind of interaction was formed between the lignin and lysine under the conditions of sonication.[55−57]

Lignin is known to possess carboxylic acid (1−8%, w/w) functional groups.[58,59] To further test our hypothesis, lysine was sonicated with either 9-anthracenecarboxylic acid or 9-anthracenemethanol to test for the feasibility of amide- or ester-bond formation under the sonication conditions (Figure 1; the details of solution preparation are available in Section S1 of the Supporting Information). Anthracene was selected as a proxy for lignin because it is a water-insoluble substrate. Accordingly, 9-anthracenemethanol (9A-OH) and 9-anthracenecarboxylic acid (9A-COOH) alone formed heterogeneous mixtures after sonication. After tip sonication with lysine, however, 9A-OH remained heterogeneous but 9A-COOH formed a stable and homogenized solution. Analysis by LC-MS revealed only the starting components and no evidence of a covalent bond between lysine and 9A-COOH (Section S2, Figure S1, and Table S1). The lysine-9A-COOH conjugate was still able to create a water-dispersible 9A-lysine-SWCNT (Figure 1D). When comparing the solubility of bare 9A-COOH and 9A-COOH-lysine in water, as can be seen, 9A-COOH-lysine is significantly more water-soluble compared to 9A-COOH alone (Figure 1). Thus, while no evidence supports an ester or amide covalent linkage between lignin and lysine, an ionic pairing between the carboxylic groups in the lignin and the ammonium groups of the lysine may contribute to the formation of stable SWCNT dispersions (*vide infra*). In contrast, there is no chemical rationale for an ionic linkage between lysine and 9A-OH, and there is no evidence of possible ester formation.

Lignin is also known to possess ketone and aldehyde carbonyl (1−2%, w/w) functional groups,[58,59] providing an avenue to form covalent imine bonds with the amino groups of lysine. Sonication of anthracene-9-carbaldehyde (A-9-CHO) with lysine produced detectable quantities of the imine product via LCMS analysis. However, the reversibility of imine formation in aqueous media meant that the imine product diminished over time (Section S2, Scheme S1, Figures S2 and S3, and Table S2), indicating that covalent bond formation between lignin and lysine is an unlikely contributor to SWCNT dispersion.

Finally, characterization of the lignin−lysine conjugate via NMR was not possible because the size of the lignin particles led to slow tumbling on the NMR time scale and loss of signal.

Collectively, these results led us to conclude that the primary interaction between lignin and lysine is ionic. The presence of hydroxyl groups in lignin (2−8%, w/w) is broadly taken for granted, but carboxylic acid groups (1−8%, w/w) are present in comparable amounts.[58,59] We propose that the sonication of lignin and lysine leads to ion pairing mediated by acid−base interactions. We further propose that this process exfoliates the lignin material, exposing hydrophobic sites for binding to the SWCNT while also increasing the solubility (Scheme 1).

3.2. Observations after Mechanochemical Coupling.

To visualize probe stability after mechanochemical coupling, the three aqueous solutions of lysine−SWCNT (without lignin), lignin−SWCNT (without lysine), and LLS after 30 min of centrifugation at 10000 rpm (11180*g*) were visualized (Figure 2). As can be seen, lysine−SWCNT and lignin−SWCNT dispersions are unstable and crash out of solution, whereas no sedimentation is observed at the bottom of the tube for the LLS solution after prolonged centrifugation, indicating the success of the coupling and solubilization process. To ensure the stability of the prepared solution, we also increased the centrifugation speed to 12000 rpm (16087*g*), but we still did not observe much difference, and the LLS solution remained stable. It is also worth mentioning that storing the LLS solution under atmospheric conditions for 30 days did not lead to any sedimentation or aggregation of the suspended nanoprobes.

Moreover, as shown in Figure 2E, centrifugation of the lignin−SWCNT solution (without lysine) resulted in the sedimentation of 70−78% (mass basis) of the lignin and SWCNT. However, the remaining lignin−SWCNT in the solution made it too dark to visually distinguish from the LLS solution (Figure 2G), which had relatively no sedimentation after centrifugation. We observed that lysine alone does not stabilize SWCNTs; instead, lignin is largely responsible for their stabilization. In other words, the presence of lysine provided highly stable lignin, which consequently stabilizes the conjugated SWCNTs. It is also worth mentioning that we observed significant lignin sedimentation when using an equimolar ratio of lysine to lignin or even a mass ratio of less than 1:1. This can be attributed to the much smaller size and fewer amine groups (two amines per lysine molecule) of lysine compared with the large lignin molecules, which contain many ketone and aldehyde carbonyl groups. Therefore, we concluded that to facilitate sufficient ion pairing between amines and carboxylic acids and covalent imine bonds between the ketone/aldehyde carbonyl functional groups in a single

https://doi.org/10.1021/acsami.4c13800
ACS Appl. Mater. Interfaces 2024, 16, 62547−62556

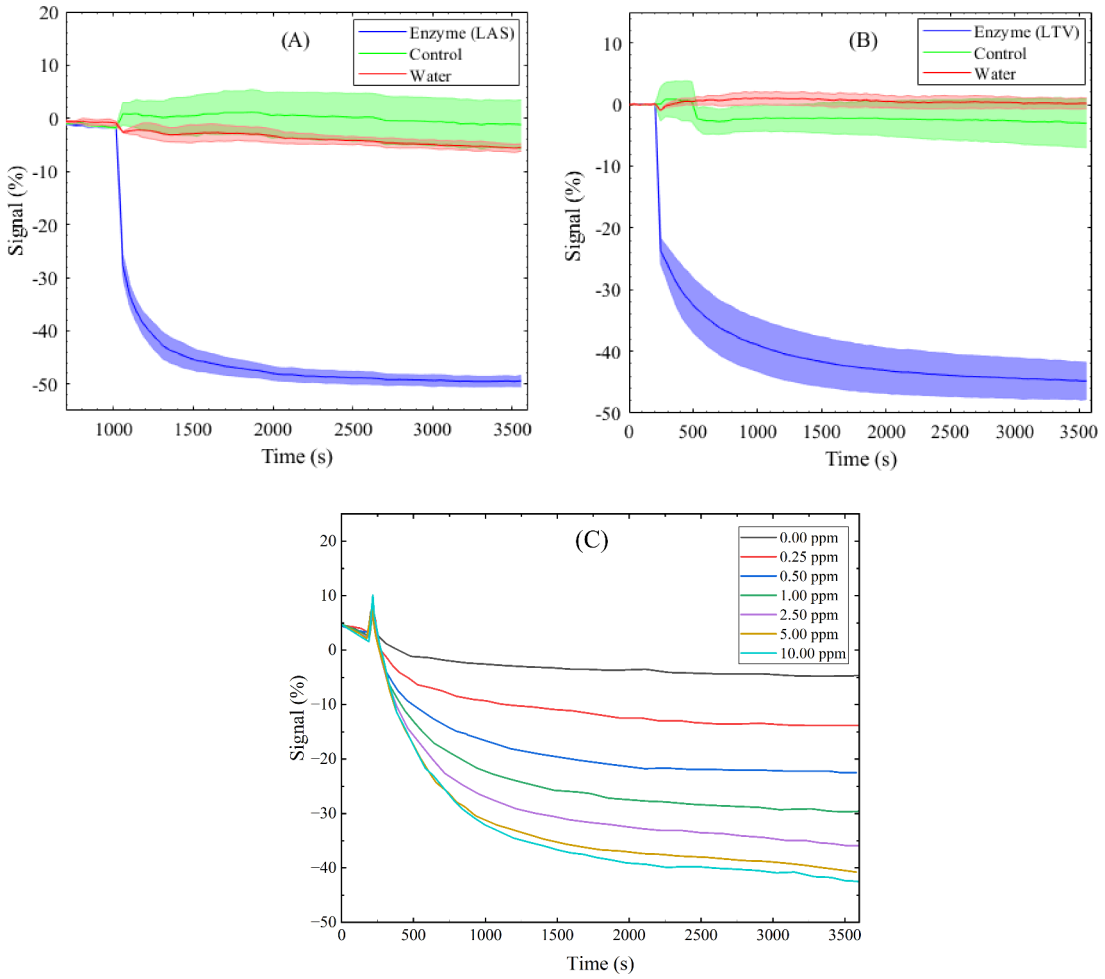

Figure 3. Response of LLS to two commercial ligninases: (A) LacAS and (B) LacTV at 40 ppm (volume basis of formulated product) with controls of heat denatured enzymes. Also, the enzyme concentration dependence of signal change for LLS to LacAS (C) exhibited detection down to 0.25 ppm (volume basis of formulated product).

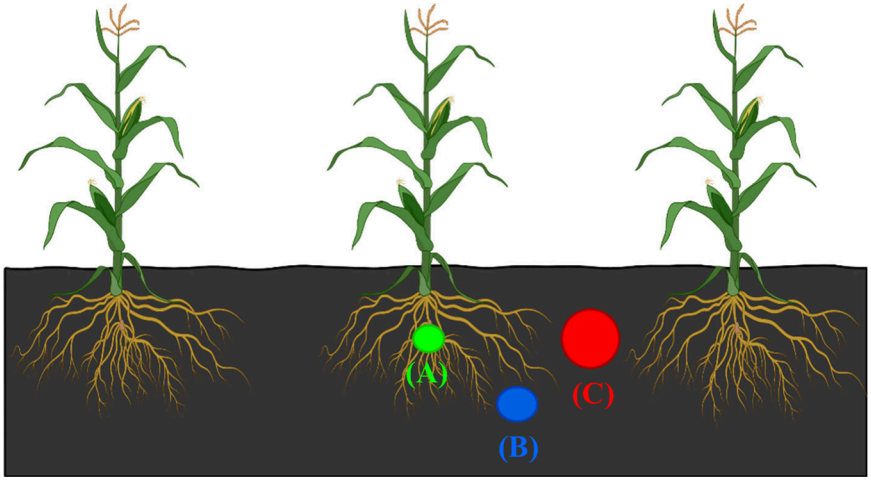

Figure 4. Showing the three soil zones sampled for method application: (A) rhizosphere, (B) row, and (C) inter-row. The "shovel-and-shake" method was used in a maize row crop system typical of Iowa, USA, to isolate soil from each of these three zones.

lignin molecule, an excess of lysine molecules is necessary. This excess provides enough pairing, resulting in a stable, water-soluble lignin.

3.3. Selectivity and Sensitivity. The sensitivity of LLS to hydrolytic degradation was checked with two well-known ligninase:[60] Laccase from Aspergillus species (LacAS, SAE0050, Sigma) and Laccase from Trametes versicolor (LacTV, 38429, Sigma). In prior nanoprobe work with amphiphilic wrappings,[16,27] upon enzyme addition there was a strong decrease in signal attributed to hydrolases attacking

https://doi.org/10.1021/acsami.4c13800
ACS Appl. Mater. Interfaces 2024, 16, 62547−62556

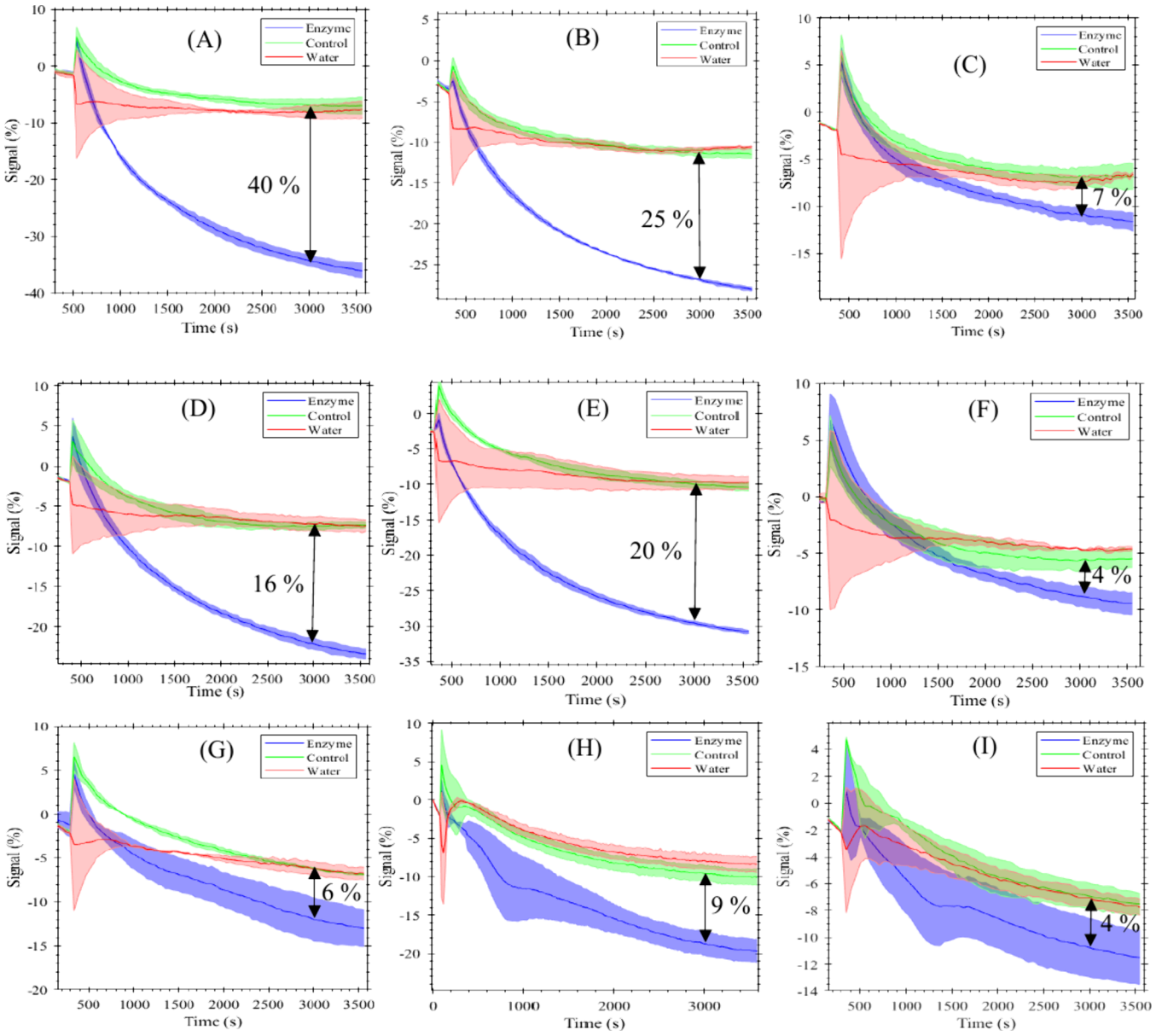

Figure 5. Response of LLS to available enzymes in (A) rhizosphere, (B) row, and (C) inter-row soil samples and the response of LLS to enzymes in rhizosphere soil samples after 2 weeks under preservation temperatures of (D) −20, (E) 4, and (F) 25 °C and after 4 weeks under preservation temperatures of (G) −20, (H) 4, and (I) 25 °C. Control samples are heat-denatured. Each condition was tested with $n = 3$ technical replicates, with one standard deviation shown in the shaded regions.

the substrate coating, increasing solvent access, and thereby quenching signal response. A similar response is observed for LLS to both types of ligninases (Figure 3A,B). However, its sensitivity was greater for LacAS, and the lignin element on SWCNT was degraded in a shorter time period (900 s after adding the ligninase solution, the signal line for LLS became relatively constant), compared to LacTV, where degradation continued even after 3500 s. Figure 3C also illustrates the response of LLS to LacAS within the concentration range of 0−10 ppm, showcasing not only the sensitivity of LLS but also its capability to quantify the proportion of ligninase compounds at low concentrations (less than 0.5 ppm on a volume basis of formulated commercial product).

3.4. Application of Probes: Measuring Soil Hydrolase Activity. Assessment of potential soil enzymatic activity was chosen as an application of this new method to demonstrate the sensitivity and utility of these probes. Soil samples were collected using the "shovel-and-shake" method[61] from three zones (Supporting Information, Section S6): (A) the rhizosphere (soil closely adhering to the plant's roots), (B) the row (under the plant roots but not directly attached), and (C) the inter-row (furthest distance from the plant's roots) (Figure 4). We sampled soil in these three zones from a research field of Zea mays (maize) that has been under consistent management practices for nearly 15 years, ensuring more stable soil enzyme profiles. According to the literature on potential enzyme activity in soil, hydrolytic enzyme activity is expected to increase the closer to the plant root, from (C) to (A) because of greater microbial biomass and greater influence of maize roots.[62,63] Consequently, it is anticipated that higher enzyme activity would be observed in the rhizosphere and lower enzyme activity would be observed in the inter-row areas. It is

https://doi.org/10.1021/acsami.4c13800
ACS Appl. Mater. Interfaces 2024, 16, 62547−62556

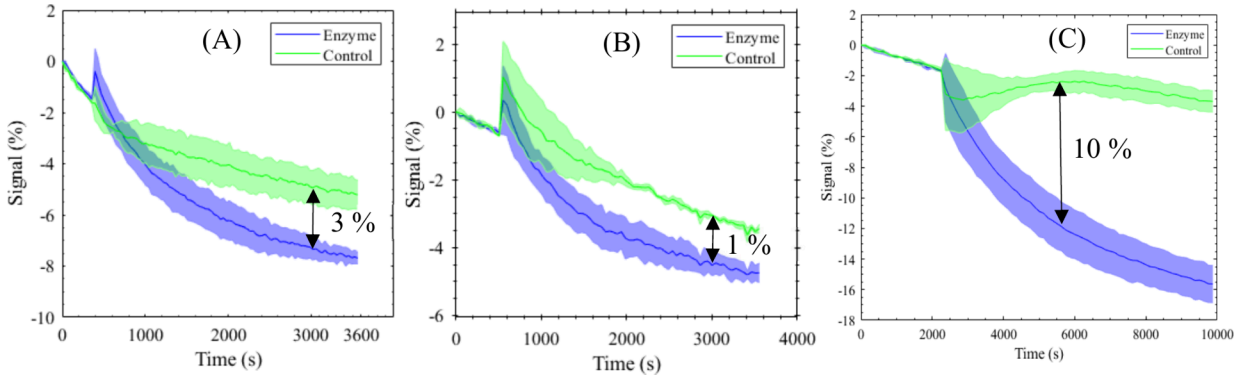

Figure 6. Response of LLS to the enzymes available in (A) Sparta, (B) Coland, and (C) Nicollet soil types. Percent decrease was displayed 3000 s after adding soil samples. Control samples are heat-denatured. Each condition was run with $n = 3$ technical replicates, and one standard deviation is shown in the shaded regions.

important to note that these sensors provide a relative measure of enzyme activity on the same soil mass basis, not a traditional enzyme turnover rate (k_{cat}) or activity of a specific enzyme type. To determine a turnover rate, one would need detailed assessment of enzyme concentration and confidence that only a single enzyme type was active (rather than a consortium of different enzymes and/or same enzymes immobilized on soil particles vs free in solution). Such assessment is beyond the reach of these sensors; however, they are capable of giving careful spatial mapping of activity across different soil regions.

The results of enzyme activity screening for inter-row, row, and rhizosphere soil samples are shown in Figure 5. To compare the enzyme activity of the soil samples, we labeled the difference between active enzymes and denatured controls as the difference index (*D*-index) at a set time point (3000 s). As can be seen, among the studied soil samples, the rhizosphere zone with a *D*-index of approximately 40% exhibited the highest level of activity compared to the row zone with 15% and the inter-row zone with 7%, thereby confirming our expected activity differences based on soil zone and literature on potential enzyme activity in relation to plant roots.[62−64]

To observe the impact of storage conditions and time on enzyme degradation, we extended the enzyme screening in the rhizosphere zone to monitor the gradual decline of the *D*-index. This was necessary because, in other areas, the enzyme activity was significantly lower, causing them to be degraded more rapidly and rendering conclusive observations impossible. Previous studies have shown some artifacts of soil storage on potential enzyme activity measured with the traditional fluoro-linked substrates and some decline with storage[65,66] and even some confounding artifacts that interact with treatments, making comparisons of stored samples somewhat challenging.[67] The rhizosphere soil samples were kept under three storage temperatures −20, 4, and 25 °C, and the enzyme activity screening analysis was performed after 2 and 4 weeks. Storing at 4 °C resulted in the least negative effect on the activity of enzymes available in soil samples compared to the storage at −20 and 25 °C; however, all stored samples showed an attenuated signal to that measured from fresh soil, indicating the importance of fast screening or field side methods, as we have attempted with these nanoprobes.[16] Degradation in storage has been attributed to instability of enzymes and aggregation as is common with other protein products.[65,66]

To assess the performance of LLS with a variety of soil textures, enzyme activity screening was conducted on fresh Nicollet soil and two soil types, Coland and Sparta, which had been stored for over four years at 25 °C and then had their enzyme activities reactivated. As illustrated in Figure 6, LLS successfully detected active enzymes in all soil samples, with the largest change observed in the fresh Nicollet samples. This indicates one potential use of spatial mapping of enzyme activity caused by varied soils that differ largely in texture, soil organic matter, water holding capacity, and cation exchange capacity,[68] not to mention their soil biological potential when substrates are added.[69] Relative to fresh soil (Figure 5A−C) and refrigerated and frozen soil (Figure 5D−I), the air-dried soil potential enzyme activity was much lower (36% signal reduction).

3.5. Modularity of Mechanochemical Approach. As another test of modularity of this method, we prepared a zein−lysine−SWCNT sensor using the same procedure as for the LLS. Zein is a water-insoluble protein derived from corn composed of many nonpolar (proline, leucine, and alanine) amino acids but also polar groups, namely, glutamic acid, that also present a carboxylic acid for ion pairing. As illustrated in Figure 7A, the coupling process was successful in producing a stable probe after centrifugation and long-term (>1 month) storage. This probe was employed to evaluate the enzyme activity of bacterial protease. In this experiment, commercial bacterial protease pellets (Carolina 202390) were dissolved in

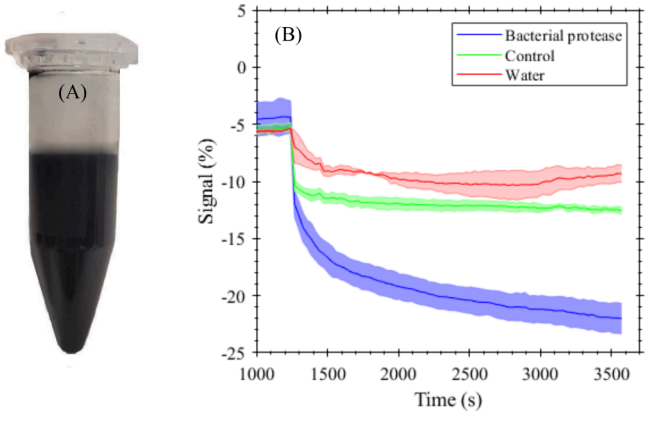

Figure 7. (A) Zein−lysine−SWCNT and (B) the response of zein−lysine−SWCNT to the bacterial protease. Control samples are heat-denatured. Each condition was run with $n = 3$ technical replicates, and one standard deviation is shown in the shaded regions.

https://doi.org/10.1021/acsami.4c13800
ACS Appl. Mater. Interfaces 2024, 16, 62547−62556

DI water (25 g/L). The resulting solution was then used along with zein−lysine−SWCNT sensor in a ratio of 20 μL of zein−lysine−SWCNT to 80 μL of bacterial protease solution, as detailed in the NIR Experiment section. The zein−lysine−SWCNT sensor effectively detected the enzyme activity in the bacterial protease solution vs a heat-denatured control (Figure 7B).

4. CONCLUSIONS

In this study, we proposed a facile, mechanochemical strategy to render hydrophobic substrates suitable for noncovalent association to SWCNT for screening hydrolase activity in aqueous buffers. This was performed by tip sonication of the target insoluble substrate in the presence of lysine, forming ion pairs between the lysine and carboxylic acid groups present on the substrate. The coupled substrates are then used to suspend the SWCNT and form a probe for hydrolase activity measurements. As a focusing application, coupled lignin−lysine-suspended SWCNT probes (LLS) measured relative enzyme activity in varied root zones and storage conditions. LLS corroborated literature precedence, such as the maximum activity in fresh samples close to the root. Another hydrophobic substrate, zein, was coupled with the same approach and made the sensor sensitive to bacterial protease. Furthermore, we verified the chemistry of the coupling process by designing a similar coupling reaction between lysine and anthracenes with a single carboxylic acid group, supporting our hypotheses regarding the N−COOH coupling to form ion pairs. The result of this work enables a large library of natural hydrophobic substrates to be rendered into soluble activity probes for high throughput screening applications such as the discovery and optimization of enzymes for valorization of biomass. In addition, applying such coupling processes, such as synthesizing LLS, could potentially benefit various fields, including water purification, heavy metal removal from water resources, energy storage, and photocatalytic manufacturing.

■ ASSOCIATED CONTENT

Data Availability Statement

All data generated or analyzed during this study are included in this published article. Raw data available upon request.

Supporting Information

The Supporting Information is available free of charge at https://pubs.acs.org/doi/10.1021/acsami.4c13800.

Sections S1−S6, Figures S1−S5, and Tables S1−S4 (PDF)

■ AUTHOR INFORMATION

Corresponding Author

Nigel F. Reuel − *Department of Chemical and Biological Engineering, Iowa State University, Ames, Iowa 50011, United States;* orcid.org/0000-0003-3438-2919; Email: reuel@iastate.edu

Authors

Abbas Elhambakhsh − *Department of Chemical and Biological Engineering, Iowa State University, Ames, Iowa 50011, United States*

Mohaddeseh Abbasi − *Department of Chemistry, Iowa State University, Ames, Iowa 50011, United States*

Cole R. Dutter − *Department of Agronomy, Iowa State University, Ames, Iowa 50011, United States;* orcid.org/0000-0002-8098-7639

Marshall D. McDaniel − *Department of Agronomy, Iowa State University, Ames, Iowa 50011, United States*

Brett VanVeller − *Department of Chemistry, Iowa State University, Ames, Iowa 50011, United States;* orcid.org/0000-0002-3792-0308

Andrew C. Hillier − *Department of Chemical and Biological Engineering, Iowa State University, Ames, Iowa 50011, United States;* orcid.org/0000-0002-2729-1368

Complete contact information is available at: https://pubs.acs.org/10.1021/acsami.4c13800

Author Contributions

A.E.: investigation, methodology, and writing−original draft. N.R.: conceptualization, visualization, supervision, project administration, writing−review and editing. M.D.M.: soil sample access and experimental design; editing of manuscript. C.R.D.: soil sample collection and data interpretation. M.A.: NMR experimental design and execution. B.V.V.: NMR experimental design and analysis and editing of manuscript. A.H.: SEM experimental design and execution.

Funding

This work was financially supported in part by NIH MIRA ESI award R35GM138265 and an ISU VPR seed grant to N.F.R. as well as NSF award 2404390 to B.V. Field access through RegenPGC is supported by Agriculture and Food Research Initiative Competitive Grant no. 2021-68012-35923 from the USDA National Institute of Food and Agriculture.

Notes

The authors declare the following competing financial interest(s): N.F.R. is a cofounder and paid director at Zymosense Inc. which seeks to commercialize SWCNT based probes for biotechnology applications, such as enzyme optimization and discovery. This advance is being pursued as IP to be licensed by Zymosense Inc. This COI is managed by an established plan at ISU.

■ ACKNOWLEDGMENTS

We express our appreciation to Stephen Potter for his vital assistance in sample collection and ancillary measurements, which contributed to the success of this research. Any opinions, findings, conclusions, or recommendations expressed in this presentation are those of the author(s) and do not necessarily reflect the view of the U.S. Department of Agriculture.

■ REFERENCES

(1) Busto, E.; Gotor-Fernández, V.; Gotor, V. Hydrolases: catalytically promiscuous enzymes for non-conventional reactions in organic synthesis. *Chem. Soc. Rev.* **2010**, *39* (11), 4504−4523.

(2) Li, S.; Yang, X.; Yang, S.; Zhu, M.; Wang, X. Technology prospecting on enzymes: application, marketing and engineering. *Computational and structural biotechnology journal* **2012**, *2* (3), No. e201209017.

(3) Kawai, F.; Kawabata, T.; Oda, M. Current state and perspectives related to the polyethylene terephthalate hydrolases available for biorecycling. *ACS Sustainable Chem. Eng.* **2020**, *8* (24), 8894−8908.

(4) Reetz, M. T.; Qu, G.; Sun, Z. Engineered enzymes for the synthesis of pharmaceuticals and other high-value products. *Nature Synthesis* **2024**, *3*, 19−32.

(5) Singh, R.; Kumar, M.; Mittal, A.; Mehta, P. K. Microbial enzymes: industrial progress in 21st century. *3 Biotech* **2016**, *6*, 1−15.
(6) Burns, R. G. Enzyme activity in soil: location and a possible role in microbial ecology. *Soil biology and biochemistry* **1982**, *14* (5), 423−427.
(7) Dick, R. P.; Burns, R. G. *Soil Enzymes-Methods of Soil Enzymology*; Wiley: 2011; Vol. *9*, pp 1−35.
(8) Allison, S. D.; Vitousek, P. M. Responses of extracellular enzymes to simple and complex nutrient inputs. *Soil Biology and Biochemistry* **2005**, *37* (5), 937−944.
(9) Geisseler, D.; Horwath, W. R. Regulation of extracellular protease activity in soil in response to different sources and concentrations of nitrogen and carbon. *Soil Biology and Biochemistry* **2008**, *40* (12), 3040−3048.
(10) Frankenberger, W., Jr.; Dick, W. Relationships between enzyme activities and microbial growth and activity indices in soil. *Soil science society of America journal* **1983**, *47* (5), 945−951.
(11) Białas, K.; Moschou, D.; Marken, F.; Estrela, P. Electrochemical sensors based on metal nanoparticles with biocatalytic activity. *Microchimica Acta* **2022**, *189* (4), 172.
(12) Dzyadevych, S. V.; Soldatkin, A. P.; Korpan, Y. I.; Arkhypova, V. N.; El'skaya, A. V.; Chovelon, J.-M.; Martelet, C.; Jaffrezic-Renault, N. Biosensors based on enzyme field-effect transistors for determination of some substrates and inhibitors. *Anal. Bioanal. Chem.* **2003**, *377*, 496−506.
(13) Teller, C.; Halámek, J.; Makower, A.; Fournier, D.; Schulze, H.; Scheller, F. A piezoelectric sensor with propidium as a recognition element for cholinesterases. *Sens. Actuators, B* **2006**, *113* (1), 214−221.
(14) Barone, P. W.; Parker, R. S.; Strano, M. S. In vivo fluorescence detection of glucose using a single-walled carbon nanotube optical sensor: design, fluorophore properties, advantages, and disadvantages. *Analytical chemistry* **2005**, *77* (23), 7556−7562.
(15) Rodríguez-Sevilla, P.; Thompson, S. A.; Jaque, D. Multichannel fluorescence microscopy: advantages of going beyond a single emission. *Advanced NanoBiomed. Research* **2022**, *2* (5), 2100084.
(16) Kallmyer, N. E.; Abdennadher, M. S.; Agarwal, S.; Baldwin-Kordick, R.; Khor, R. L.; Kooistra, A. S.; Peterson, E.; McDaniel, M. D.; Reuel, N. F. Inexpensive Near-Infrared Fluorometers: Enabling Translation of nIR-Based Assays to the Field. *Anal. Chem.* **2021**, *93* (11), 4800−4808.
(17) Qi, J.; Liu, D.; Liu, X.; Guan, S.; Shi, F.; Chang, H.; He, H.; Yang, G. Fluorescent pH sensors for broad-range pH measurement based on a single fluorophore. *Analytical chemistry* **2015**, *87* (12), 5897−5904.
(18) Lv, Y.; Zhou, Z.; Shen, Y.; Zhou, Q.; Ji, J.; Liu, S.; Zhang, Y. Coupled fluorometer-potentiostat system and metal-free monochromatic luminophores for high-resolution wavelength-resolved electrochemiluminescent multiplex bioassay. *ACS sensors* **2018**, *3* (7), 1362−1367.
(19) Pu, L. Simultaneous determination of concentration and enantiomeric composition in fluorescent sensing. *Acc. Chem. Res.* **2017**, *50* (4), 1032−1040.
(20) Wang, X.; Hu, J.; Zhang, G.; Liu, S. Highly selective fluorogenic multianalyte biosensors constructed via enzyme-catalyzed coupling and aggregation-induced emission. *J. Am. Chem. Soc.* **2014**, *136* (28), 9890−9893.
(21) Fang, H.; Chen, Y.; Jiang, Z.; He, W.; Guo, Z. Fluorescent probes for biological species and microenvironments: from rational design to bioimaging applications. *Acc. Chem. Res.* **2023**, *56* (3), 258−269.
(22) Kompa, J.; Bruins, J.; Glogger, M.; Wilhelm, J.; Frei, M. S.; Tarnawski, M.; D'Este, E.; Heilemann, M.; Hiblot, J.; Johnsson, K. Exchangeable HaloTag ligands for super-resolution fluorescence microscopy. *J. Am. Chem. Soc.* **2023**, *145* (5), 3075−3083.
(23) Jiao, Z.; Yang, C.; Zhou, Q.; Hu, Z.; Jie, J.; Zhang, X.; Su, H. Sequence-specific binding behavior of coralyne toward triplex DNA: An ultrafast time-resolved fluorescence spectroscopy study. *J. Chem. Phys.* **2023**, *158*, 045101.
(24) Basu, S.; Hendler-Neumark, A.; Bisker, G. Monitoring Enzyme Activity Using Near-Infrared Fluorescent Single-Walled Carbon Nanotubes. *ACS sensors* **2024**, *9* (5), 2237−2253.
(25) Kruss, S.; Hilmer, A. J.; Zhang, J.; Reuel, N. F.; Mu, B.; Strano, M. S. Carbon nanotubes as optical biomedical sensors. *Advanced drug delivery reviews* **2013**, *65* (15), 1933−1950.
(26) Kuo, M.-T.; Raffaelle, J. F.; Waller, E. M.; Varaljay, V. A.; Wagner, D.; Kelley-Loughnane, N.; Reuel, N. F. Screening enzymatic degradation of polyester polyurethane with fluorescent single-walled carbon nanotube and polymer nanoparticle conjugates. *ACS Nano* **2023**, *17* (17), 17021−17030.
(27) Agarwal, S.; Kallmyer, N. E.; Vang, D. X.; Ramirez, A. V.; Islam, M. M.; Hillier, A. C.; Halverson, L. J.; Reuel, N. F. Single-walled carbon nanotube probes for the characterization of biofilm-degrading enzymes demonstrated against Pseudomonas aeruginosa extracellular matrices. *Analytical chemistry* **2022**, *94* (2), 856−865.
(28) Koman, V. B.; Bakh, N. A.; Jin, X.; Nguyen, F. T.; Son, M.; Kozawa, D.; Lee, M. A.; Bisker, G.; Dong, J.; Strano, M. S. A wavelength-induced frequency filtering method for fluorescent nanosensors in vivo. *Nat. Nanotechnol.* **2022**, *17* (6), 643−652.
(29) Hendler-Neumark, A.; Wulf, V.; Bisker, G. In vivo imaging of fluorescent single-walled carbon nanotubes within C. *elegans nematodes in the near-infrared window. Materials Today Bio* **2021**, *12*, 100175.
(30) Wulf, V.; Bisker, G. Single-walled carbon nanotubes as fluorescent probes for monitoring the self-assembly and morphology of peptide/polymer hybrid hydrogels. *Nano Lett.* **2022**, *22* (22), 9205−9214.
(31) Basu, S.; Hendler-Neumark, A.; Bisker, G. Rationally Designed Functionalization of Single-Walled Carbon Nanotubes for Real-Time Monitoring of Cholinesterase Activity and Inhibition in Plasma. *Small* **2024**, *20*, 2309481.
(32) Chandna, S.; Olivares, C. A. M.; Baranovskii, E.; Engelmann, G.; Boker, A.; Tzschucke, C. C.; Haag, R. Lignin Upconversion by Functionalization and Network Formation. *Angew. Chem., Int. Ed.* **2024**, *63* (8), No. e202313945.
(33) Cateto, C. A.; Barreiro, M. F.; Rodrigues, A. E.; Belgacem, M. N. Optimization study of lignin oxypropylation in view of the preparation of polyurethane rigid foams. *Ind. Eng. Chem. Res.* **2009**, *48* (5), 2583−2589.
(34) Fabbri, F.; Bischof, S.; Mayr, S.; Gritsch, S.; Jimenez Bartolome, M.; Schwaiger, N.; Guebitz, G. M.; Weiss, R. The biomodified lignin platform: a review. *Polymers* **2023**, *15* (7), 1694.
(35) Su, Y.-T.; Wang, G.-W. FeCl3-mediated cyclization of [60] fullerene with N-benzhydryl sulfonamides under high-speed vibration milling conditions. *Org. Lett.* **2013**, *15* (13), 3408−3411.
(36) Do, J.-L.; Friščić, T. Mechanochemistry: a force of synthesis. *ACS central science* **2017**, *3* (1), 13−19.
(37) Martinez, V.; Stolar, T.; Karadeniz, B.; Brekalo, I.; Užarević, K. Advancing mechanochemical synthesis by combining milling with different energy sources. *Nature Reviews Chemistry* **2023**, *7* (1), 51−65.
(38) James, S. L.; Adams, C. J.; Bolm, C.; Braga, D.; Collier, P.; Friščić, T.; Grepioni, F.; Harris, K. D.; Hyett, G.; Jones, W.; et al. Mechanochemistry: opportunities for new and cleaner synthesis. *Chem. Soc. Rev.* **2012**, *41* (1), 413−447.
(39) Banerjee, S.; Hawthorne, N.; Batteas, J. D.; Rappe, A. M. Two-Legged Molecular Walker and Curvature: Mechanochemical Ring Migration on Graphene. *J. Am. Chem. Soc.* **2023**, *145* (49), 26765−26773 2023.
(40) Stanojkovic, J.; William, R.; Zhang, Z.; Fernández, I.; Zhou, J.; Webster, R. D.; Stuparu, M. C. Synthesis of precisely functionalizable curved nanographenes via graphitization-induced regioselective chlorination in a mechanochemical Scholl Reaction. *Nat. Commun.* **2023**, *14* (1), 803.
(41) Wang, G.-W. Mechanochemical organic synthesis. *Chem. Soc. Rev.* **2013**, *42* (18), 7668−7700.

https://doi.org/10.1021/acsami.4c13800
ACS Appl. Mater. Interfaces 2024, 16, 62547−62556

(42) Hernández, J. G.; Friščić, T. Metal-catalyzed organic reactions using mechanochemistry. *Tetrahedron Lett.* **2015**, *56* (29), 4253−4265.
(43) Ayoub, G.; Karadeniz, B.; Howarth, A. J.; Farha, O. K.; Đilović, I.; Germann, L. S.; Dinnebier, R. E.; Uzarevic, K.; Friscic, T. Rational synthesis of mixed-metal microporous metal-organic frameworks with controlled composition using mechanochemistry. *Chem. Mater.* **2019**, *31* (15), 5494−5501.
(44) Karadeniz, B.; Žilić, D.; Huskić, I.; Germann, L. S.; Fidelli, A. M.; Muratović, S.; Lončarić, I.; Etter, M.; Dinnebier, R. E.; Barišić, D.; et al. Controlling the polymorphism and topology transformation in porphyrinic zirconium metal-organic frameworks via mechanochemistry. *J. Am. Chem. Soc.* **2019**, *141* (49), 19214−19220.
(45) Sun, J.; Wang, X.; Wang, Q.; Peng, L.; Liu, Y.; Wei, D. Ultrafast supercritically solvothermal polymerization for large single-crystalline covalent organic frameworks. *Nat. Protoc.* **2023**, 1−34.
(46) Lu, Y.; Sugita, H.; Mikami, K.; Aoki, D.; Otsuka, H. Mechanochemical reactions of Bis (9-methylphenyl-9-fluorenyl) peroxides and their applications in cross-linked polymers. *J. Am. Chem. Soc.* **2021**, *143* (42), 17744−17750.
(47) Krusenbaum, A.; Grätz, S.; Tigineh, G. T.; Borchardt, L.; Kim, J. G. The mechanochemical synthesis of polymers. *Chem. Soc. Rev.* **2022**, *51* (7), 2873−2905.
(48) Xiao, Y.; Wu, C.; Hu, X.; Chen, K.; Qi, L.; Cui, P.; Zhou, L.; Yin, Q. Mechanochemical Synthesis of Cocrystal: From Mechanism to Application. *Cryst. Growth Des.* **2023**, *23* (6), 4680−4700.
(49) Bolla, G.; Sarma, B.; Nangia, A. K. Crystal engineering of pharmaceutical cocrystals in the discovery and development of improved drugs. *Chem. Rev.* **2022**, *122* (13), 11514−11603.
(50) Teoh, Y.; Ayoub, G.; Huskić, I.; Titi, H. M.; Nickels, C. W.; Herrmann, B.; Friščić, T. SpeedMixing: Rapid tribochemical synthesis and discovery of pharmaceutical cocrystals without milling or grinding media. *Angew. Chem., Int. Ed.* **2022**, *61* (41), No. e202206293.
(51) Pan, H.; Liu, L.; Guo, Z.-X.; Dai, L.; Zhang, F.; Zhu, D.; Czerw, R.; Carroll, D. L. Carbon nanotubols from mechanochemical reaction. *Nano Lett.* **2003**, *3* (1), 29−32.
(52) Yang, Z.; Kuang, W.; Tang, Z.; Guo, B.; Zhang, L. Generic mechanochemical grafting strategy toward organophilic carbon nanotubes. *ACS Appl. Mater. Interfaces* **2017**, *9* (8), 7666−7674.
(53) Fantozzi, N.; Volle, J.-N.; Porcheddu, A.; Virieux, D.; García, F.; Colacino, E. Green metrics in mechanochemistry. *Chem. Soc. Rev.* **2023**, *52*, 6680−6714.
(54) Naidu, B. R.; Sruthi, T.; Mitty, R.; Venkateswarlu, K. Catalyst-free mechanochemistry as versatile tool in synthetic chemistry: a review. *Green Chem.* **2023**, *25*, 6120−6148.
(55) Martínez, R. F.; Cravotto, G.; Cintas, P. Organic sonochemistry: a chemist's timely perspective on mechanisms and reactivity. *Journal of organic chemistry* **2021**, *86* (20), 13833−13856.
(56) Nam, Y. T.; Choi, J.; Kang, K. M.; Kim, D. W.; Jung, H.-T. Enhanced stability of laminated graphene oxide membranes for nanofiltration via interstitial amide bonding. *ACS Appl. Mater. Interfaces* **2016**, *8* (40), 27376−27382.
(57) Jia, J.; Gai, Y.; Wang, W.; Zhao, Y. Green synthesis of biocompatiable chitosan-graphene oxide hybrid nanosheet by ultrasonication method. *Ultrasonics sonochemistry* **2016**, *32*, 300−306.
(58) El Mansouri, N.-E.; Salvadó, J. Analytical methods for determining functional groups in various technical lignins. *Industrial crops and products* **2007**, *26* (2), 116−124.
(59) Argyropoulos, D. D.; Crestini, C.; Dahlstrand, C.; Furusjö, E.; Gioia, C.; Jedvert, K.; Henriksson, G.; Hulteberg, C.; Lawoko, M.; Pierrou, C.; et al. Kraft Lignin: A Valuable, Sustainable Resource, Opportunities and Challenges. *ChemSusChem* **2023**, *16* (23), No. e202300492.
(60) Asemoloye, M. D.; Marchisio, M. A.; Gupta, V. K.; Pecoraro, L. Genome-based engineering of ligninolytic enzymes in fungi. *Microbial Cell Factories* **2021**, *20*, 1−18.
(61) Gomes, N. C. M.; Fagbola, O.; Costa, R.; Rumjanek, N. G.; Buchner, A.; Mendona-Hagler, L.; Smalla, K. Dynamics of fungal communities in bulk and maize rhizosphere soil in the tropics. *Applied and environmental microbiology* **2003**, *69* (7), 3758−3766.
(62) Zhang, X.; Dippold, M. A.; Kuzyakov, Y.; Razavi, B. S. Spatial pattern of enzyme activities depends on root exudate composition. *Soil Biology and Biochemistry* **2019**, *133*, 83−93.
(63) Ma, X.; Liu, Y.; Zarebanadkouki, M.; Razavi, B. S.; Blagodatskaya, E.; Kuzyakov, Y. Spatiotemporal patterns of enzyme activities in the rhizosphere: effects of plant growth and root morphology. *Biology and Fertility of Soils* **2018**, *54*, 819−828.
(64) Curtright, A. J.; Tiemann, L. K. Intercropping increases soil extracellular enzyme activity: a meta-analysis. *Agriculture, ecosystems & environment* **2021**, *319*, 107489.
(65) DeForest, J. L. The influence of time, storage temperature, and substrate age on potential soil enzyme activity in acidic forest soils using MUB-linked substrates and L-DOPA. *Soil Biology and Biochemistry* **2009**, *41* (6), 1180−1186.
(66) Lane, J. M.; Delavaux, C. S.; Van Koppen, L.; Lu, P.; Cade-Menun, B. J.; Tremblay, J.; Bainard, L. D. Soil sample storage conditions impact extracellular enzyme activity and bacterial amplicon diversity metrics in a semi-arid ecosystem. *Soil Biology and Biochemistry* **2022**, *175*, 108858.
(67) Peoples, M. S.; Koide, R. T. Considerations in the storage of soil samples for enzyme activity analysis. *Applied soil ecology* **2012**, *62*, 98−102.
(68) Nelson, J. T.; Adjuik, T. A.; Moore, E. B.; VanLoocke, A. D.; Ramirez Reyes, A.; McDaniel, M. D. A Simple, Affordable, Do-It-Yourself Method for Measuring Soil Maximum Water Holding Capacity. *Commun. Soil Sci. Plant Anal.* **2024**, *55*, 1190−1204.
(69) De, M.; Sawyer, J. E.; McDaniel, M. D. Crude glycerol, a biodiesel byproduct, used as a soil amendment to temporarily immobilise and then release nitrogen. *European Journal of Soil Science* **2022**, *73* (3), No. e13241.

https://doi.org/10.1021/acsami.4c13800
ACS Appl. Mater. Interfaces 2024, 16, 62547−62556